

Improved flat plate collector with heat pipes for overheating prevention in solar thermal systems

Bert Schiebler¹, Finn Weiland¹, Federico Giovannetti¹, Oliver Kastner¹, Steffen Jack²

¹ Institut für Solarenergieforschung Hameln (ISFH), Am Ohrberg 1, 31860 Emmerthal (Germany)

² KBB Kollektorbau GmbH, Bruno-Bürgel-Weg 142-144, 12439 Berlin (Germany)

Abstract

Heat pipes in solar thermal collectors can reduce thermal loads in the solar circuit by using the physical effect of dry-out limitation. By avoiding high temperatures and vapor formation, simplified, more reliable and cost effective solar thermal systems can be designed. This paper presents a theoretical study on different heat pipe and manifold configurations for flat plate collectors. The focus is on a high thermal efficiency in the operating range and a significant temperature limitation in stagnation mode. Several prototype collectors are manufactured and experimentally investigated by means of indoor performance measurements. Thereby, a conversion factor of 73 % is reported, which represents an increase of 4 percentage points compared to a previous prototype. During stagnation events we localize a maximum fluid temperature about 130 °C within the manifold, which decreases to values below 100 °C towards the collector connections. Finally, we evaluate the system performance of the prototype with an exemplary solar DHW-system by means of dynamic TRNSYS-simulations. The results show that the calculated annual yield is predicted only 5 % lower than the one of a comparable direct flow collector and critical stagnation events can be fully avoided.

Keywords: heat pipe, stagnation temperature, overheating prevention, flat plate collector

1. Introduction

Heat pipes in solar thermal collectors are commercially used in combination with evacuated tube collectors (ETC). Heat pipe-based flat plate collectors (FPC) so far have only been realized within research projects, see Jack et al. (2014). In comparison to direct flow collectors, the heat pipe design incorporates additional thermal resistances into the heat transport path of the collector, which results from the heat pipe process between fluid evaporation along the absorber section and fluid condensation in the manifold section as well as heat transfer resistances between the adjacent collector parts (Schiebler et al. 2018a). Elevated heat transport capabilities in the heat pipes and good thermal connections to the solar circuit at the manifold section are important for high overall collector efficiencies. Figure 1 shows the principle design with the manifold being located in the upper part of the device. This design leads to an unfavorable aperture/gross area ratio compared to typical direct flow FPC.

An essential advantage of heat pipe collectors is the fact that the heat transport is internally interrupted during stagnation events, when the solar heat is not absorbed by the exterior solar circuit due to limited demand. Technically, this intrinsic fallback system is related to a dry-out effect of the heat pipes at situations of over-heating, where the two-phase flow and thus the heat transport are interrupted. This shut-off behavior can be designed by proper choice of the working fluid and its amount enclosed in the heat pipe under vacuum conditions.

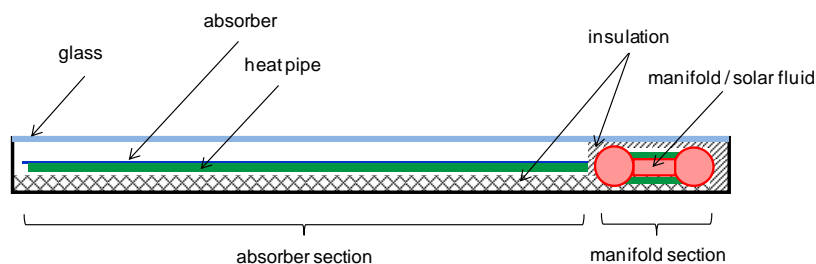


Fig. 1: Schematic longitudinal section of a flat plate collector with heat pipes

In a previous work, the maximum temperature in the solar circuit has been successfully limited to 140 °C by using an innovative heat pipe-based FPC (Jack et al., 2014). The measured zero-loss coefficient η_0 amounts to 69 %. The current development aims at the optimization of the performance in the operating range as well as the reduction of the shut-off temperature to 125 °C. By such a temperature limitation the evaporation of the solar fluid can be completely avoided during stagnation, as we have already demonstrated with heat pipe-based ETC (Schiebler et al. 2017). The avoidance of vapor formation increases the general operational safety of the system, thus reducing the design requirements to the other components of the solar circuit (smaller expansion vessel, use of polymers, etc.). As a result, the reliability of the overall system is increased and both investment and maintenance costs can be significantly reduced. The present paper reports improvements achieved with a new prototype: After characterizing the thermal efficiency of the collector we analyze its stagnation behavior and the system performance compared to an identical, direct flow FPC.

2. Heat transfer of the heat pipe – manifold connection

The heat pipe condenser-manifold connection is already state-of-the-art in ETC and commercially available in different design variants. Typically, the cylindrical condensers are attached to a shaped manifold pipe (Figure 2), which is transversely perfused by the solar fluid. Because of higher heat losses of FPC devices in comparison to evacuated collectors in general, the thermal heat transfer between absorber and manifold gains superior importance to achieve elevated collector efficiencies.

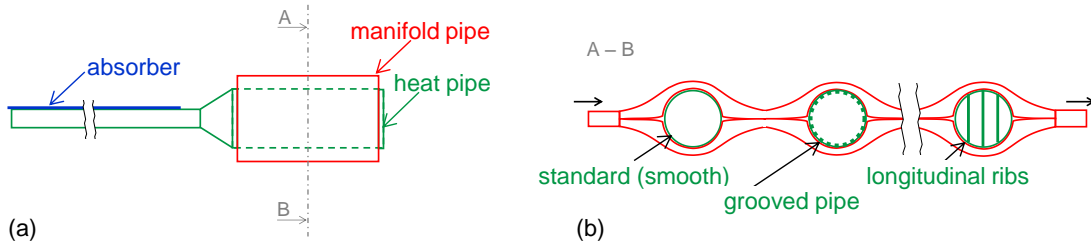


Fig. 2: Schematic drawing of a typical manifold for ETC with different heat pipe variations (smooth, grooved, with ribs). (a) Side view, (b) Cross-section A-B

We employ the internal heat transfer coefficient U_{int} as design parameter to qualify the thermal connection between the absorber plate and the solar circuit fluid. For heat pipe-based FPC, this quantity is related to three partial heat transfer mechanisms indicated in Figure 3: Conductive transport of the absorbed solar heat through the absorber plate towards the heat pipe, characterized by the partial transfer coefficient U_{abs} , heat transport through the heat pipe cycle towards the manifold section (U_{hp}) and heat transfer from the heat pipe towards the manifold (U_{man}). The heat transfer U_{hp} through the heat pipe may specified into the contributions of the evaporation section (U_{evap}) and the condensation section (U_{cond}), and the heat transfer from condenser to the manifold by the contributions of the contact interface ($U_{contact}$), the conductive heat transfer through the manifold pipe material (U_{mp}) and the heat transfer into the solar circuit fluid ($U_{\alpha,mp}$). Note that for direct flow collectors, U_{int} is reduced to the contributions of U_{abs} and U_{man} , where the latter represents the heat transfer from the absorber plate towards the solar circuit fluid running through pipes in direct thermal contact with the absorber.

Both the heat pipe and the manifold have to be considered for optimization purpose. The influence of the heat transfer from the heat pipe to the solar circuit fluid on the thermal efficiency of the whole collector is expressed by the conversion factor η_0 according to Equation 1 and 2,

$$\eta_0 = (\tau\alpha)_{eff} \cdot \frac{U_{int}}{U_{int} + U_{loss}} \quad (eq. 1)$$

$$1/U_{int} = 1/(n_{hp} \cdot U_{abs}) + 1/(n_{hp} \cdot U_{hp}) + 1/(n_{hp} \cdot U_{man}) \quad (eq. 2)$$

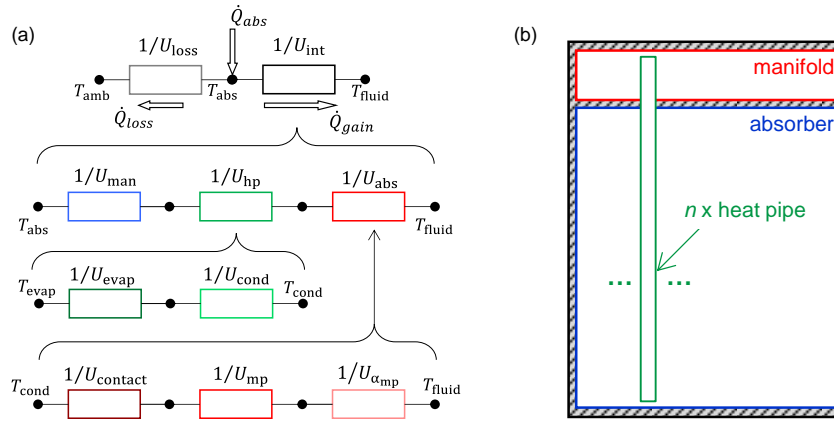


Fig. 3: (a) Composition of the internal heat transfer coefficient on the basis of the individual thermal resistances of absorber, heat pipe and manifold in the heat flow path of the collector. (b) Schematic representation of heat transfer coefficients of a heat pipe-based FPC

To achieve a conversion factor of $\eta_0 = 75\%¹$, this equations may be used to calculate the required U_{man} (with reference to aperture area) in dependency of U_{hp} and the number of heat pipes in the collector (see Figure 4 (a)). To optimize the heat pipe process, we investigate the use of inner grooved pipes and condenser pipes with longitudinal ribs (see Figure 2 and 4, (b)). An inner grooved pipe surface can improve the heat transfer in the operating range, but also influences the dry-out behavior of the heat pipes (Föste et al., 2016), as discussed in Section 4.4 on the basis of the collector efficiency curve.

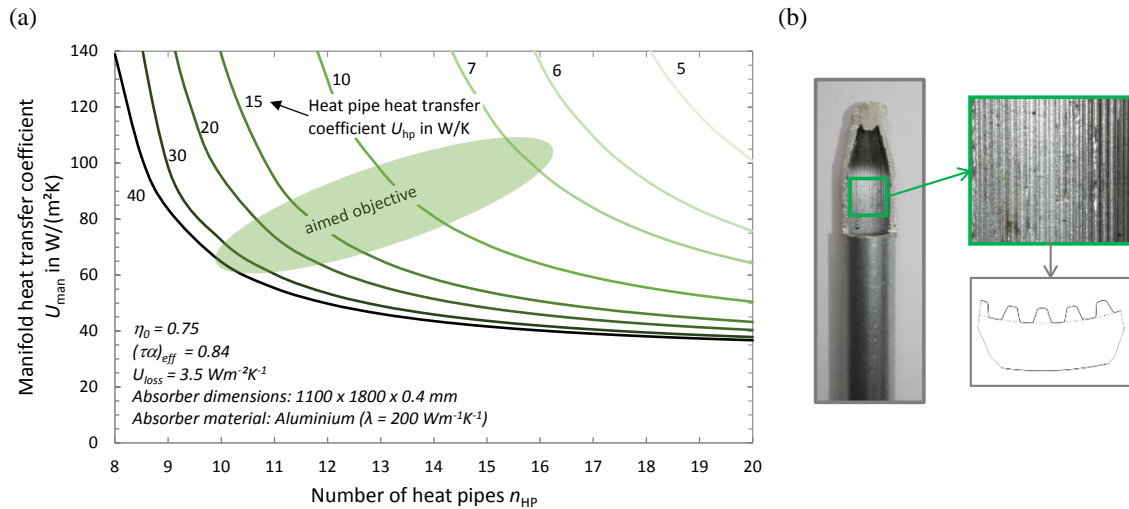


Fig. 4: (a) Required manifold heat transfer coefficient U_{man} versus the heat pipe heat transfer coefficient U_{hp} and the number of heat pipes in the collector to achieve a conversion factor of 75 %. (b) Illustration of the considered grooved aluminum pipes.

In the sequel we investigate three collector concepts (A, B, C), which differ by type and design of the thermal connection. Design variant (C) represents a commercial ETC manifold depicted in Figure 2, which is considered as reference design. The two concepts (A) and (B) suggest comparatively simpler manifold designs. These manifold designs consist of three, respectively five, parallel cylindrical (A_{1-2}) or flat (B_{1-4}) fluid channels, which are welded to the heat pipes. The specific design cannot be given here for patenting reasons.

To predict the manifolds performance and analyze the influences of geometric and physical variations, we carry out a preliminary FEM simulation study with the commercial software COMSOL Multiphysics (see COMSOL, 2011). Depending on the concept, we vary the inner surface of the heat pipes evaporator and condenser (smooth and grooved internal surface, or with ribs) as well as the number of heat pipes and

¹aimed objective in the current activities

manifold pipes in the collector. The FEM simulations yields heat transfer coefficients, which are implemented into an integral collector model based on Equation 1, used to evaluate the overall collector efficiency. The results show that the conversion factor η_0 of all three concepts (A-C) ranges between 72 and 75 %, indicating tangible improvement of a previous prototype ($\eta_0 = 69 %$), see Figure 5. The concepts (B₁) and (B₂) are based on heat pipes without complex diameter expansion (see d_{cond} in Table 1) and have a high thermal performance even without inner-grooved or finned heat pipes.

Tab. 1: Properties of the considered manifold concepts A-C

Manifold concept	A ₁	A ₂	B ₁	B ₂	B ₃	B ₄	C ₁	C ₂	C ₃
Evaporator diameter d_{evap} in mm	8.0	8.0	8.0	8.0	8.0	8.0	8.0	8.0	8.0
Condenser diameter d_{cond} in mm	18.0	18.0	8.0	8.0	8.0	8.0	20.0	20.0	20.0
Number of heat pipes n_{hp}	11	11	11	11	11	11	15	15	15
Number of manifold pipes n_{mp}	3	5	3	5	3	5	2	2	2
U_{hp} in W/m ² K (calculated)	195 ¹	195 ¹	82.1	82.1	154 ²	154 ²	35.0	63 ³	63 ²
U_{man} in W/m ² K (calculated)	31.4	36.3	53.4	58.0	53.4	58.0	75.8	75.8	75.8

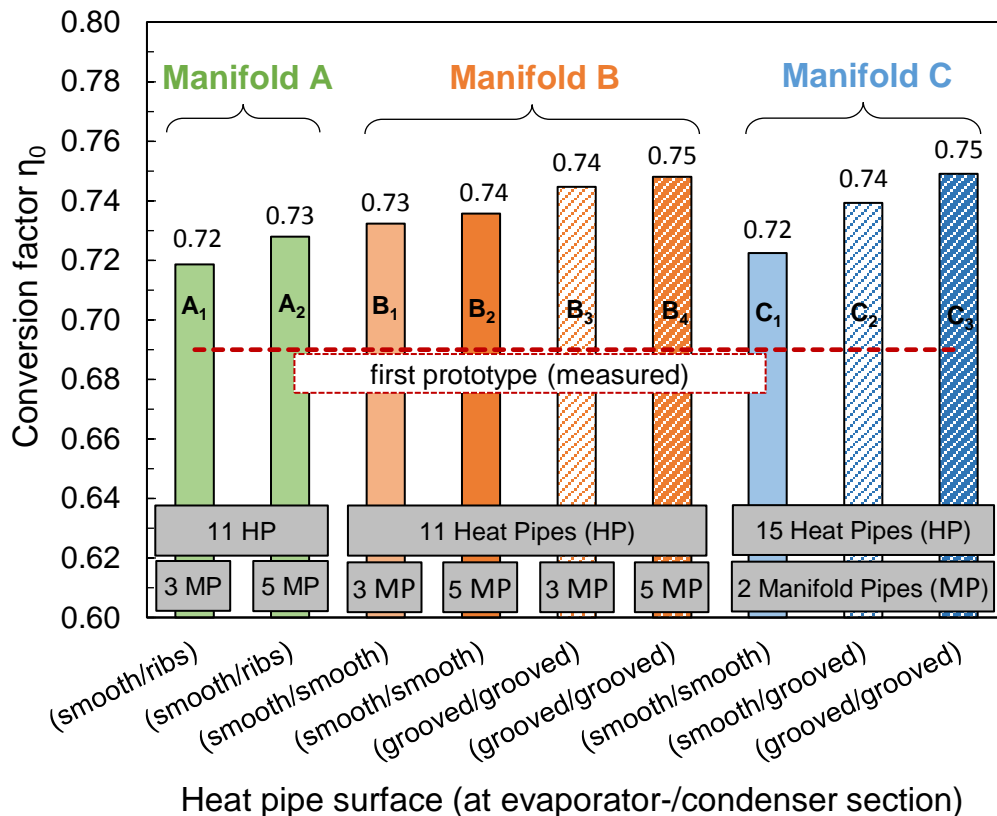


Fig. 5: Simulated conversion factors η_0 for the investigated manifold designs as function of the design parameters “inner tube surface” (smooth, grooved, with longitudinal ribs) and “number of manifold pipes” (n_{mp})

¹with longitudinal ribs at the condenser

²with grooved pipes at the evaporator and condenser as Figure 4 (a)

³with grooved pipes only at the condenser

3. Experimental evaluation of a heat pipe collector prototype

3.1 Performance testing

Based on design concept (B₁) a collector prototype was manufactured by the German company KBB Kollektorbau GmbH using aluminum heat pipes filled with 4-5 g butane as working fluid. A typical FPC-housing was used, whereby three configurations are realized: Configuration 1 is equipped with a standard glass cover and a fully insulated manifold, see Table 2. Configuration 2 uses a glass cover with anti-reflex coating (AR). Configuration 3 omits the insulation at the manifold section. The collector efficiency, the heat losses and the shut-off behavior are evaluated by indoor sun simulator testing according to ISO 9806 (2018). The collectors are equipped with additional temperature sensors to investigate the individual heat transfer coefficients of the heat pipe process as well as the connection to the manifold.

Tab. 2: Test results of the three collector configuration prototypes.

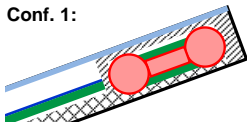
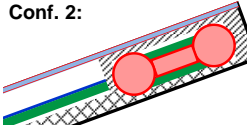
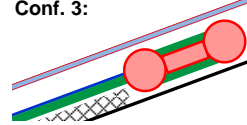
		Conf. 1:	Conf. 2:	Conf. 3:
				
specifications		standard glass cover and fully insulated manifold	anti-reflex coating (AR glass cover) and fully insulated manifold	manifold without insulation
η_0	-	0.733	0.762	0.762
a_1	W/m ² K	3.562	3.615	4.260
a_2	W/m ² K ²	0.017	0.017	0.017
T_{\max}^1	°C	130	130	106

Figure 6 shows the measured heat transfer rate of an individual heat pipe as function of the average fluid temperature (orange line color). Within the heat pipe operating range up to a fluid temperature of 66 °C, the curve progresses like a typical FPC, indicating increasing heat losses with temperature. The average heat transfer coefficient of a single heat pipe U_{hp} is detected as 16 W/K in this temperature range. Thus, the calculated heat pipe heat transfer coefficient, as reported in Table 1, could be experimental validated. Considering the number of parallel heat pipes at the collector ($n_{hp} = 11$) and its aperture area ($A_{ap} = 2,15 \text{ m}^2$), the overall heat pipe heat transfer coefficient amounts to 82 W/m²K. The heat transfer coefficient of the manifold U_{man} is with 46 W/m²K smaller than expected (see Table 1). The overall internal heat transfer coefficient U_{int} is 23 W/m²K. In comparison, U_{int} of common direct flow FPC range between 60 and 80 W/m²K. We see that the heat pipe heat transfer coefficient U_{hp} exhibits an elevated level compared to U_{man} . Note that U_{hp} can be almost doubled to about 30 W/K using internally grooved pipes (Figure 4(b)), Föste et al. (2015). The manifold heat transfer coefficient U_{man} , which represents the highest thermal resistance in the heat flow path of the collector, offers the most relevant potential for further optimizations.

¹measured in stagnation mode (solar irradiation $G = 990 \text{ W/m}^2$, ambient temperature $T_{amb} = 26 \text{ °C}$, no wind and no fluid mass flow)

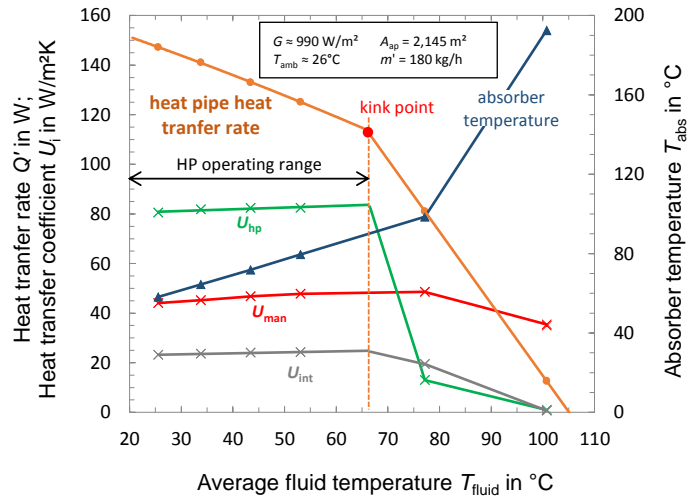


Fig. 6: Progression of the heat pipe heat transfer rate (orange curve), the heat transfer coefficients of the heat pipes U_{hp} (green) and of the manifold U_{man} (red), the overall internal heat transfer coefficient U_{int} (grey) and resulting absorber temperature (blue) as function of the average fluid temperature during laboratory tests. The dry-out effect sets in beyond the kink point indicated.

3.2 Collector efficiency curve

The measured conversion factors of the prototype ranges between 73.3 % with standard class cover (Configuration 1) and 76.2 % with AR class cover (Configuration 2), see Table 2 and Figure 7. Compared to the heat pipe FPC prototype reported by Jack et al., (2014), this indicates an efficiency increase of 4.3 percentage points. Using internally grooved heat pipes, a further increase of about 2 percentage points is expected. As already seen in Figure 6, the collector performance sharply decays at an average fluid temperature above 66 °C. This is also reflected by the efficiency curve of Figure 7, which compares the measured prototype efficiencies of configurations 1-3. For temperatures above 66 °C, the collector power quickly shuts-off as a result of the heat pipes dry-out effect. This power shut-off is very well described by the increase of the linear heat loss coefficient from about 3.6 in the operating range to 15 W/m²K at higher temperatures. For comparison, the efficiency curve of an identical direct flow FPC is indicated by a solid line in Figure 7.

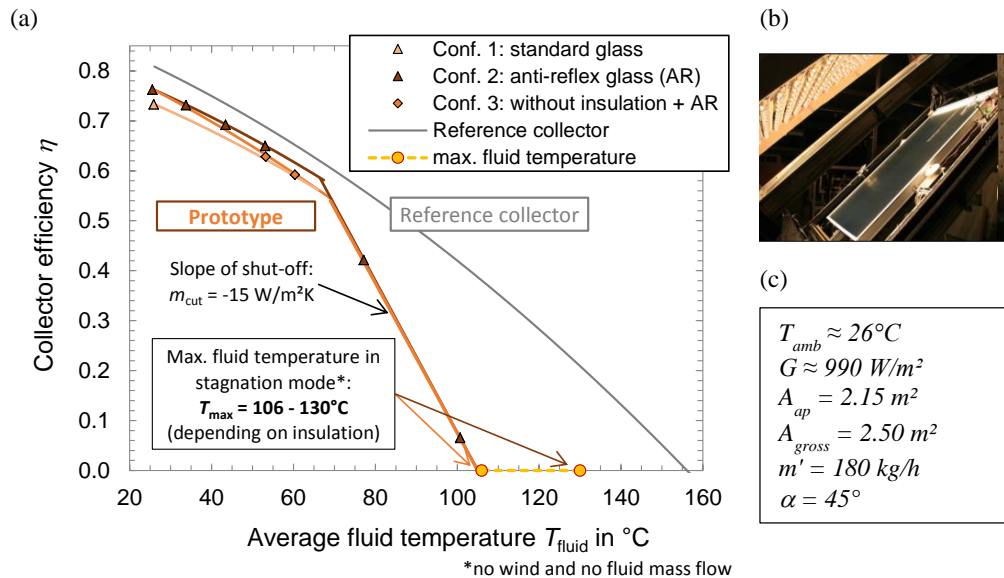


Fig. 7: (a) Efficiency curve of the prototype collectors (Configurations 1-3, colored lines) in comparison to a direct flow collector (reference, grey line) as function of the average fluid temperature. (b) One of the prototypes during laboratory tests situated in the sun simulator device of ISFH. (c) Test conditions

3.2 Stagnation mode

The shut-off temperature of the collector depends on the heat pipes dry-out effect and on the thermal insulation at the manifold section. In stagnation mode, transport of absorber heat to the solar circuit fluid is reduced to axial thermal conductivity along the metal pipe walls. In order to limit this contribution, the thermal losses at the manifold section may be increased by omitting the insulation. Stagnation tests yield maximum fluid temperatures of 106 °C (for Configuration 3) and 130 °C (for Configurations 1 and 2) in the manifold pipes. Close to the collector connections, the temperature drops below 100 °C in all cases (see Figure 8). This means that the heat pipe related power shut-off prevents undesired evaporation of the solar circuit fluid during stagnation largely. This effect has to be compared to typical stagnation temperatures of direct flow FPC (180 - 200 °C) and related vapor productions.

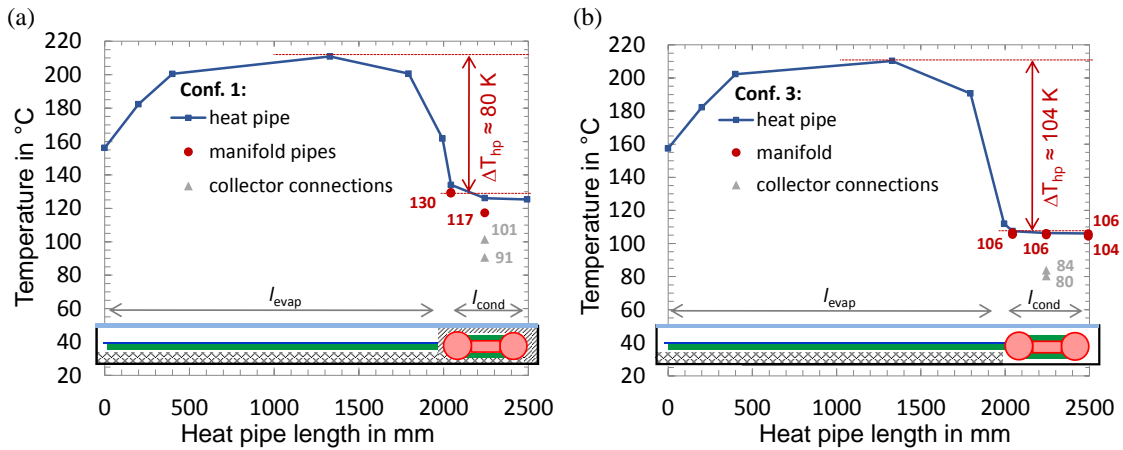


Fig. 8: Axial temperature distributions during stagnation for Configuration 2 (a) and Configuration 3 (b).

4. Simulation study in TRNSYS

4.1 Simulation setup

We simulate annual solar yields for a representative solar thermal system using the TRNSYS suite. Because of the specific heat pipe characteristics, standard collector models cannot be used for this purpose. Therefore an existing TRNSYS collector type (Type 832) has been modified so as to represent the heat pipe power shut-off effect, based on a two-temperature-node model, which allows evaluating the absorber temperature as well as the commonly evaluated fluid temperature. The power shut-off process is included by implementing an additional power function into the existing TRNSYS collector type. The function used for this purpose two parameters, their significance shown in Figure 9: the slope m_{cut} of the efficiency section indicating the power shut-off. This parameter corresponds to the linear heat loss coefficient during the heat pipes dry-out process. And furthermore the maximum fluid temperature T_{cut} at $\eta = 0$. T_{cut} represents the maximum temperature of the heat pipe process, which is independent of the manifold insulation. Hence the heat pipes dry-out limit is integrated as a simple linear function.

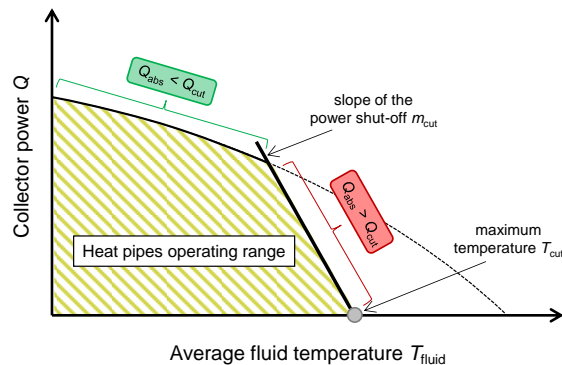


Fig. 9: Linear modeling of the power shut-off process using the slope of the dry-out limit m_{cut} as well as the maximum temperature T_{cut}

The dynamic system simulations consider a solar assisted domestic hot water system (DHW) with 5 m² gross collector area and 300 l water storage (see Figure 10) according to Bachmann et al. (2018). We simulate the system performance for different collector coefficients using the parameters of the prototype collectors as well as the parameters of an identical but direct flow reference FPC of Table 3. Configurations 1 to 3 assume smooth heat pipes (see prototype measurement in Section 3) and Configuration 4 inner-grooved heat pipes. The system efficiency is evaluated on the basis of the saved final energy E_t according to IEA TASK 54, see Louvet et al. (2018). In the following, E_t is simply referred to as the annual yield.

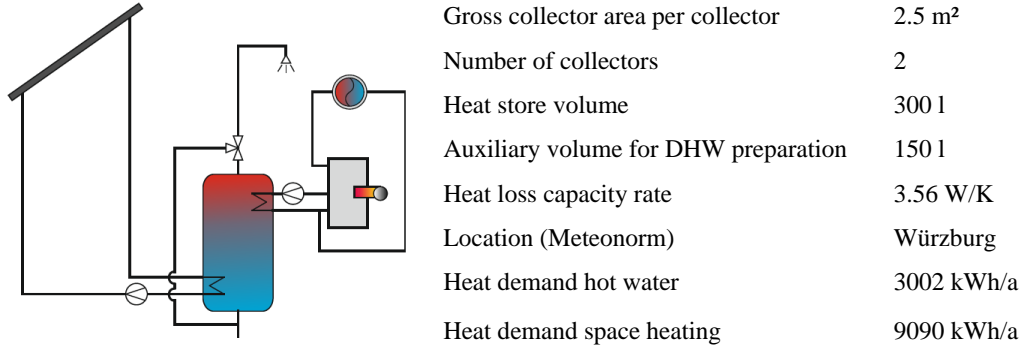


Fig. 10: Schematic view of the system configuration (left) and main system parameters (right) as reported by Bachmann et al. (2018)

Tab. 3: Collector parameters of reference and prototype collectors Conf. 1-4 based on aperture area A_{ap}

	conversion factor η_0	linear heat loss coefficient a_1 / m_{cut}	quadratic heat loss coefficient a_2	max. fluid temperature T_{cut}	specific heat capacity c_{fluid} / c_{abs}	collector area A_{ap} / A_{gross}
	-	W/m ² K	W/m ² K ²	°C	kJ/m ² K	m ²
Reference ¹	0.809	3.940	0.0170	-	3.35/2.80	2.30/2.51
Conf. 1	0.733	3.562/15 ²	0.0171	105	1.35/4.90	2.15/2.51
Conf 2	0.762	3.615/15 ²	0.0170	105	1.35/4.90	2.15/2.51
Conf 3	0.762	4.260/15 ²	0.0170	105	1.35/4.90	2.15/2.51
Conf. 4	0.749	3.466/11 ²	0.0188	110	1.35/4.90	2.15/2.51

4.2 Simulation results

Figure 11 shows the simulated annual yields of Configurations 1 and 2, compared to the reference collector. The annual yield of Configuration 1 (standard glass cover) results into 2,342 kWh/a, which is only 121 kWh/a (4.9 %) lower than the reference collector. In the case of Configuration 2 (AR glass cover) the deviation is reduced to 43 kWh/a (1.7 %), thanks to the higher solar transmittance of the glass cover. Note that the reference collector exhibits only a standard glass cover.

Considering significantly reduced conversion factors η_0 of the heat pipe prototypes, the indicated deviations of the system performances are lower than expected. This might be due to the lower specific heat capacity of the heat pipe collectors, as reported in Schiebler et al. (2017). Under transient conditions (e.g. rapid change in solar irradiation), the heat pipe system runs more frequently than that with reference collectors, which has a higher thermal inertia.

¹as specified by TÜV-Rheinland (2017)

²linear heat loss coefficient of the collector as slope of the heat pipe power shut-off (m_{cut})

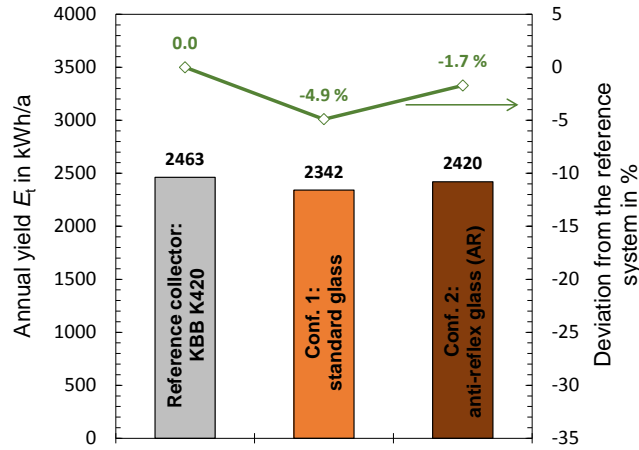


Fig. 11: Annual yield of Conf. 1 and Conf. 2 and its relative deviation compared to the reference collector

The results of the stagnation tests show that the reduction of the thermal insulation in the manifold section can reduce the maximum fluid temperatures T_{max} (see Section 3.2). As already mentioned, above the maximum temperature of the heat pipe process T_{cut} , a remaining heat flux is transferred by thermal conductance along the pipe axis. Thus the combined impact of the insulation properties of the manifold housing and the heat pipe shut-off procedure should be analyzed. Both effects should take into account designing collectors with a more convenient temperature limitation, which is aimed at unifying the maximum temperatures $T_{max} = T_{cut}$.

Beside the influences on the maximum fluid temperature in stagnation mode, elevated heat losses at the manifold section of the heat pipe also result into lower collector efficiencies in the operating range. On the basis of our experimental investigations (see Section 3), we made a theoretical study by varying the linear heat loss coefficient a_l as an important parameter of the prototype collectors. Thus, a_l ranges between 3.30 and 4.20 W/m²K, because of more or less thermal insulation in the manifold section. Figure 12 (a) illustrates the resulting collector efficiency curves, whereby the curve with $a_l = 3,56$ W/m²K represents the measured case of Configuration 1. The curve with $a_l = 4.20$ W/m²K corresponds to Configuration 3 with absent thermal insulation at the manifold section. The other curves are only theoretical based. As shown in Figure 12 (b), a higher heat loss coefficient generally leads to lower annual yields. An increase from 3.56 to 4.20 W/m²K reduce the annual yield by 48 kWh/a. The relative deviation compared to the reference collector is increased from -4.9 to -6.8 %, whereby the maximum temperature during stagnation T_{max} can be further reduced (see Figure 8). With the purpose to find an optimum compromise between insulation and power shut-off, a linear heat loss coefficient of about 3.90 W/m²K and a maximum temperature between 110 and 120 °C in stagnation mode are aimed in the scope of upcoming activities.

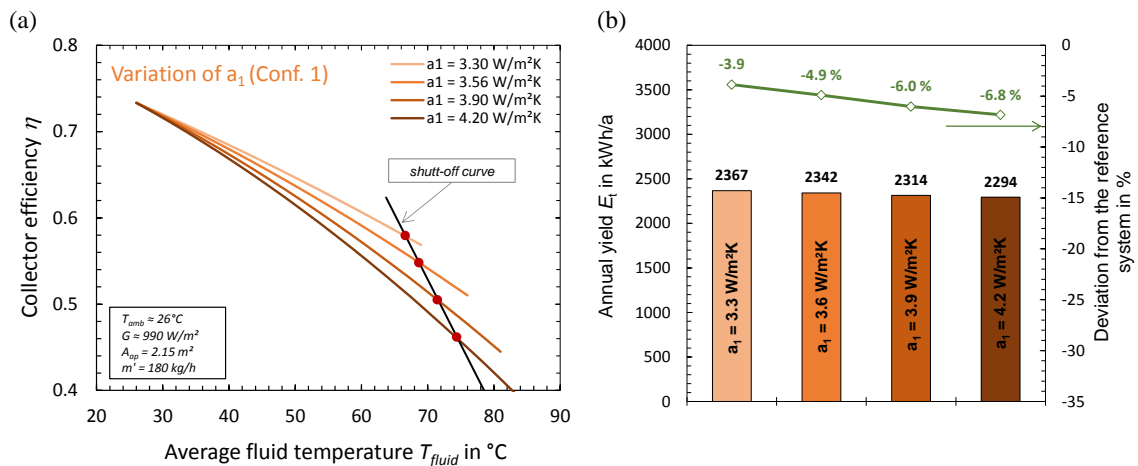


Fig. 12: (a) Different collector efficiency curves in dependency of the linear heat loss coefficient a_l . (b) Simulated annual yields as well as the relative deviations compared to the reference collector.

The power shut-off temperature of heat pipe collectors T_{cut} depends on several conditions. As reported in Schiebler et al. (2018a), the type and amount of working fluid, which is inside the heat pipe, are the most important parameters. As a general rule, lesser fluid leads to lower maximum temperatures. A temperature shift by about ± 10 K can be simply managed by properly dosing the mass of a selected fluid in the heat pipe. Another important parameter is the slope of the collector power shut-off m_{cut} , which affects the kink point and therefore the collector efficiency in the operating range. The slope of power shut-off can be influenced, e.g. by the type of working fluid and inner pipe surface (smooth/grooved).

In Figure 13, T_{cut} is varied for Configuration 1 (smooth heat pipes) and Configuration 4 (grooved heat pipes). The slope of power shut-off m_{cut} of Configuration 1 was measured as $15 \text{ W/m}^2\text{K}$ (see Section 3). In the case of grooved heat pipes (Configuration 4), the dry-out limit is experimentally determined as $11 \text{ W/m}^2\text{K}$. This means that, for identical values of T_{cut} , the kink point of Configuration 4 is significantly lower than the one of Configuration 1. As a consequence, the collector behavior in the operating range of Configuration 4 is much stronger affected by the shut-off process.

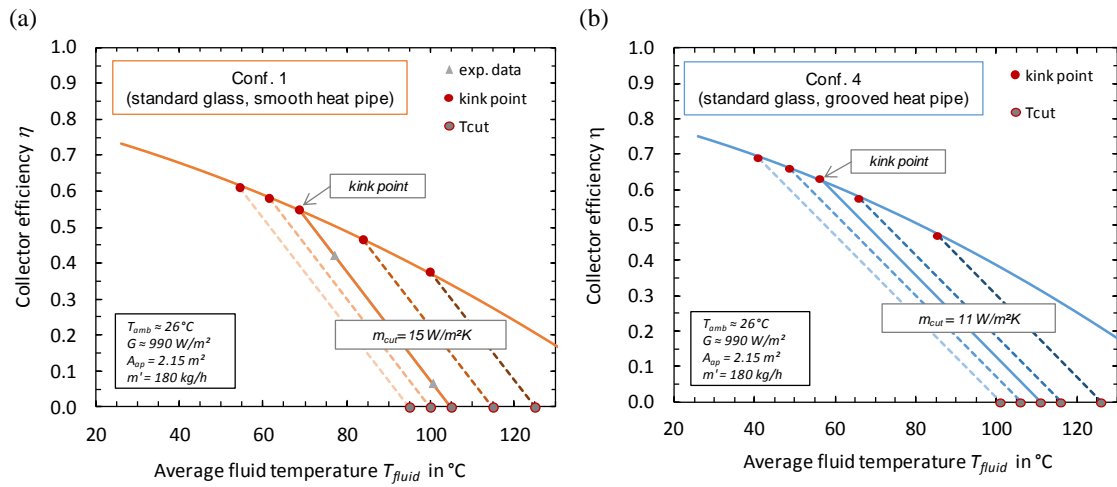


Fig. 13: (a) Collector efficiency curve with variation of the maximum temperature T_{cut} for Configuration 1 with smooth heat pipes. (b) Configuration 4 with grooved heat pipes

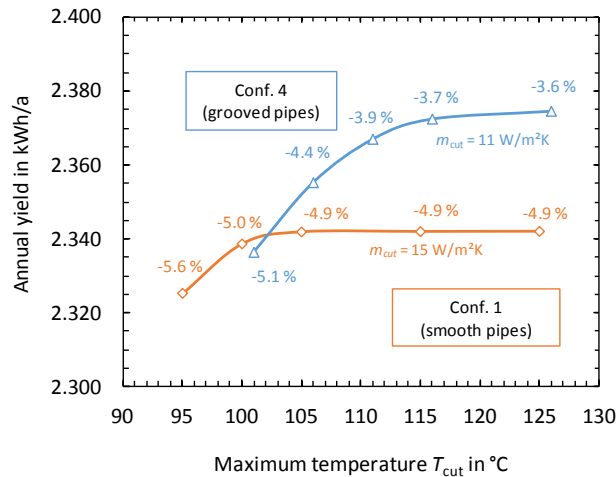


Fig. 14: Annual yield for Configuration 1 (smooth heat pipes) and Configuration 4 (grooved heat pipes) by varying the shut-off temperature T_{cut}

Figure 14 shows the results of the annual yield by varying the shut-off temperature T_{cut} . For high values as $T_{cut} \approx 125 \text{ }^\circ\text{C}$, Configuration 4 shows a significant higher annual yield of about 30 kWh/a compared to Configuration 1. For lower maximum temperatures, the kink point also shifts to lower temperatures as shown in Figure 13, which leads to a stronger impact on the collector efficiency. Configuration 1 shows a significant drop in the annual yield at $T_{cut} \approx 100 \text{ }^\circ\text{C}$. In the case of Configuration 4 this decrease occurs at $T_{cut} \approx 112 \text{ }^\circ\text{C}$. At $T_{cut} \approx 102 \text{ }^\circ\text{C}$, both configurations achieve the same annual yield, despite the higher

conversion factor of Configuration 4. Below this value, there is no significant benefit from grooved heat pipes.

In the case of Configuration 1, for temperatures T_{cut} above 105 °C the annual yields are constant, which means that the heat pipe-based power shut-off process has no influence on the system performance. The deviation of -4.9 % compared to the annual yield of the system with reference collectors is exclusively due to the additional thermal resistances of the heat pipe collector (lower internal heat transfer coefficient U_{int}). Consequently, simpler yield forecasts for heat pipe collectors in solar thermal systems, which are comparable in type and size to the considered system, can be carried out even without taking the power shut-off process into account (this assumption applies only to smooth heat pipes as in Configuration 1).

5. Conclusion and outlook

We have investigated different manifold concepts for connecting heat pipes with the solar circuit in FPC and evaluated their thermal efficiency as well as the possibility of integration in a typical FPC-housing. One of the considered designs was realized as prototype and tested in the laboratory at ISFH. The conversion factor was measured to 73.3 % (standard glass cover) and 76.2 % (AR glass cover). Compared to the results with a heat pipe-based FPC developed in a previous work, this is an improvement of 4.3 percentage points. The use of heat pipes with internal grooves further increase the conversion factor η_0 by 2 percentage points, whereby this advantage is partially compensated in the system performance by the significantly flatter slope of the power shut-off process, which negatively affects the collector efficiency in the operating range. In addition to the performance, we investigated the collector behavior under stagnation conditions. Depending on the insulation level at the manifold, the maximum collector temperature ranges between 106 and 130 °C, values which are significantly lower than the usual stagnation temperatures of collectors with direct flow (180 – 200 °C).

Furthermore we carried out annual yield simulations in TRNSYS to evaluate the system performance in dependency of the measured collector parameters and the heat pipe-based power shut-off. For a typical solar DHW-system in Würzburg, the annual yield with prototype collector is only slightly below the yield of a system an identical but direct flow reference collector. Depending on the concrete design of the prototype (insulation, heat pipes and glass cover), the yield reduction is between 1 and 7 %. As a main result of the study, it has been shown that the annual yield with standard heat pipes (no grooves) is not affected by the power shut-off process for temperatures T_{cut} above 105 °C. In such cases, the heat pipe power shut-off can be neglected and a simple collector model can be used for annual yield simulations.

As consequence of the already achieved limitation of the maximum temperature and of the successful suppression of vapor formation, system components such as the expansion vessel or the solar piping can be resized or made by cheaper polymeric materials. As described in Schiebler et al. (2018b), further cost reductions can be reached in the installation process, e.g. by the simpler filling and flushing of heat pipe collectors. For the considered DHW-system according to the IEA TASK 54 definition, a reduction of the investment costs of 9 - 19 % is expected. As another result of the significantly lower thermomechanical stress, a reduction in the annual maintenance costs of about 50 % can also be expected, which is mainly due to the increased service life of the solar circuit fluid (Schiebler et al. 2018c). The Levelized Cost of Solar Heat (LCoH_{sol}) of such a DHW-system with heat pipe collectors, which represent the cost of the produced solar energy (€/kWh) over the lifetime of the system, can be reduced by up to 26 % compared to a similar system with identical direct flow FPC.

Within the scope of this report, we considered various prototype configurations, which differ in the conversion factor, the heat loss coefficient or the power shut-off behavior. The influences on the system performance in a typical DHW-system and the corresponding maximum temperatures in stagnation mode were illustrated and comprehensively discussed. However, a detailed cost analysis is necessary for a holistic evaluation of the heat pipe-based FPC-configurations. Both the respective effort of the collector production and the individual benefits in the system costs (depending on solar yield and maximum temperature) has to be considered. Such an analysis as well as a verification of the expected cost benefits has to be proven on the basis of real systems in practice and is a part of our current activities.

6. Acknowledgement

The project "Cost effective and reliable solar systems with novel heat pipe collectors" underlying this publication was funded by the state of Lower Saxony and the German Federal Ministry of Economy and Energy (reference number 0325550A-C), following a decision of the German Parliament. The investigations are carried out in cooperation with the companies KBB Kollektorbau GmbH, NARVA Lichtquellen GmbH & Co. KG and AkoTec Produktionsgesellschaft mbH.

The authors are grateful for the support. The responsibility for the content of this publication lies with the authors.

7. References

Bachmann S., Fischer S., Furbo S., Haffner B., 2018. Definition of the reference solar domestic hot water (SDHW) system, Germany. IEA TASK 54 Info Sheet A08.

COMSOL Multiphysics GmbH, 2011. COMSOL Multiphysics User's Guide Version 4.2a, Cambridge.

Föste S., Schiebler B., Giovannetti F., Rockendorf G., Jack S., 2015. Butane heat pipes for stagnation temperature reduction of solar thermal collectors, Energy Procedia 91 p. 35-41.

ISO 9806, 2018: Solar energy – Solar thermal collectors – Test methods. Beuth Verlag, Berlin.

Jack S., Parzefall J., Luttmann T., Giovannetti F., 2014. Flat plate aluminium heat pipe collector with inherently limited stagnation temperature. Energy Procedia 48 p. 105-113.

Louvet Y., Fischer S., Furbo S., Giovannetti F., Köhl M., Mauthner F., Mugnier D., Phillippen D., Veynandt F., 2018. Guideline for levelized cost of heat (LCoH) calculations for solar thermal applications. IEA TASK 54 Info Sheet A01.

Mientkewitz G., Zabel J., 2010. Möglichkeiten eines Heatpipe-Kollektors ohne Stagnationsprobleme. Conference proceedings 20. OTTI Symposium Thermische Solarenergie, Bad Staffelstein.

Reay D.A., Kew P.A., 2006. Heat Pipes: Theory, Design and Applications. 5th edition, Butterworth Heinemann, Oxford.

Schiebler B., Weiland F., Giovannetti F., 2017. Experimental evaluation of evacuated tube collectors with heat pipes to avoid stagnation loads in a domestic hot water system, SHC/SWC Conference, Abu Dhabi 29.10.-03.11.2017.

Schiebler B., Jack S., Dieckmann H., Giovannetti F., 2018a. Experimental and theoretical investigations on temperature limitation in solar thermal collectors with heat pipes: Effect of superheating on the maximum temperature, Solar Energy 171 p. 271-278, <https://doi.org/10.1016/j.solener.2018.06.036>.

Schiebler B., Giovannetti F., Fischer S., 2018b. Levelized Cost of Heat for Solar Thermal Systems with Overheating Prevention - Info Sheet B05, IEA SHC TASK 54.

Schiebler B., Giovannetti F., Fischer S., 2018c. Reduction of Maintenance Costs by Preventing Overheating - Info Sheet B03, IEA SHC TASK 54.

Schiebler B., Giovannetti F., Schaffrath W., Jack S., 2018d. Kostengünstige und zuverlässige Solarsysteme durch neuartige Wärmerohr-Kollektoren, final project report (published in german), FKZ 0325550A-C.

TÜV-Rheinland, 2017. Solar KEYMARK Certificate, Licence Number 011-7S1683 F. DIN CERTCO, Berlin.